Asian Journal of Chemistry; Vol. 28, No. 3 (2016), 520-524

ASIAN JOURNAL OF CHEMISTRY

http://dx.doi.org/10.14233/ajchem.2016.19392

Syntheses, Bioactivity and DNA-Binding Studies of Yttrium(III) Complex

FENG-YING CHEN[1,2], ZHEN-GUO JIN[2] and SHUI-YANG HE[1,*]

[1]Laboratory of Synthetic and Natural Functional Molecule Chemistry of Ministry of Education, College of Chemistry and Materials Science, Northwest University, Xi'an 710069, Shaanxi Province, P.R. China
[2]Shaanxi Key Laboratory of Comprehensive Utilization of Tailings Resources, College of Chemical Engineering and Modern Materials, Shangluo University, Shangluo 726000, Shaanxi Province, P.R. China

*Corresponding author: E-mail: xdchemistry411@126.com

Received: 6 June 2015; *Accepted*: 31 August 2015; *Published online*: 5 December 2015; AJC-17643

Yttrium(III) complex with N-(2-propionic acid)-salicyloyl hydrazone ($C_{10}H_{10}N_2O_4$, H_3L) has been prepared and characterized. Absorption and fluorescence spectra have been carried out on the interaction of Y(III) complex with N-(2-propionic acid)-salicyloyl hydrazone $[Y_2(HL)_2(HL)_2(H_2O)][Y(HL)(H_2O)_5{\cdot}3H_2O]$ with DNA. The biological activities test shows that the compound has strong antimicrobial activity against *Botrytis cinerea Pers.ex Tris.*, *Alternaria alternata Fries keissler* and *Puccinia striiformis Westendorp.*

Keywords: Yttrium(III), Complex, DNA, Bioactivity.

INTRODUCTION

The DNA-binding metal complexes have been extensively studied as DNA structural probes, DNA-dependent electron transfer probes and so on during the past decade [1-4]. DNA-binding small molecules have since long attracted interest because of their interference with important mechanisms in the cell, some inducing mutations and cancer, while others have found use as cancer therapeutics [5]. Small molecules recognizing specific DNA sequences have attracted great interest for gene-targeted drugs, which may alter the local structure of DNA to inhibit access of activators or repressors to regulate ultimate gene expression processes [6]. The interaction of lanthanide metal complexes, containing multidentate aromatic ligands, with DNA has recently gained much attention following the important biological and medical roles [7,8].

Metal complexes of aroylhydrazones are found to have broad applications in biological processes such as in the treatment of tumour, tuberculosis, leprosy and mental disorders [9]. They are also known to act as herbicides and insecticides [10]. Specifically for the identification of hydrazones are extensively used in both synthetic and analytical chemistry. They are also employed in the polymer industry and in the pharmaceutical industry [11,12]. Recent results have indicated that this type of ligand, while coordinating with lanthanide(III), can improve biological and pharmaceutical activities due to forming special structure with lanthanide(III) [13]. Therefore, it is decided to prepare the complex of yttrium(III) with (N-(2-propionic acid)-salicyloyl hydrazone, H_3L) and to study the interaction with calf thymus-DNA by absorption spectrum, fluorescence and bioactivity measurements and its crystal structure also has been determined by X-ray diffraction analyses in order to investigate the pharmaceutical implications in the complex structure.

EXPERIMENTAL

Calf thymus DNA were purchased from Sigma (USA). The yttrium(III) nitrate was prepared by dissolving Y_2O_3 in concentrated HNO_3, then crystallizing the products. Pyruvic acid is biochemical reagent and all other chemicals used were of analytical grade.

Physical measurements: Carbon, hydrogen and nitrogen were analyzed on a PE-2400 elemental analyzer. Infrared spectra (4000-400 cm^{-1}) were obtained with KBr pellet on a EQUINOX 55 spectrometer. The ultraviolet spectra were recorded on a Lambda 40P UV-visible spectrophotometer. Fluorescence measurements were determined at room temperature using a F-4500 fluorescence spectrophotometer equipped with quartz cuvettes of 1 cm path length.

Preparation of complex: The ligand H_3L and $Y(NO_3)_3{\cdot}nH_2O$ in 2:1 (molar ratio) were dissolved in mixed solution of aqua-ethanol respectively and then mixed. The resultant solution was refluxed then filtered. The filtrate was left to evaporate naturally for about 3 weeks at room temperature and yellow prism crystals were obtained [14]. Anal. calcd. for $C_{15}H_{21}N_3O_{10.50}Y$: C 36.05, H 4.13, N 8.41; Found C 36.15, H 4.03, N 8.39.

X-ray measurements: A brilliant yellow crystal of the Y-complex (0.36 mm × 0.41 mm × 0.29 mm) was mounted on a Bruker Smart-1000 CCD diractometer and determined with graphite monochromated MoK_α radiation (0.071073 nm) using the ψ-ω scan technique at 273(2) K. The structures were refined with SHELXL-97 by full-matrix least-squares on F^2. The Y atom was located from a direct function and the other non-hydrogen atoms from Fourier synthesis. The positions of hydrogen atoms were obtained from the difference Fourier map. Routine Lorentz and polarization corrections were applied and an absorption correction was performed using semi-empirical method for compounds. The final refinement gave R1 = 0.0451, wR2 = 0.0986, GOF = 1.050.

Growth rate method: Two pathogenic microbes were used to test the biological potentials of the complex. They were *Botrytis cirerea Pers.ex Tris.* and *Alternaria alternata Fries keissler*. Antimicrobial activity of each sample was qualitatively determined by a growth rate method. The culture medium was prepared by mixing 1 mL DMF and water stock solution of the complex and 9 mL potato dextrose agar (PDA) and spreading evenly in petri dishes. Some lawns of 4 mm diameter micro-organisms were prepared by puncher under sterile conditions. The fungi lawns with mycelium downward were then carefully placed on the culture medium surface. The petri dishes were headed up and incubated for 2 days at 20 °C. Antimicrobial activity was indicated by the presence of clear inhibition zones around the fungi lawn.

Spore sprout method: *Puccinia striiformis Westendorp* pathogenic microbe was used to determine the antimicrobial activities of the ternary complex by spore spout method. Suspensions of microorganism spore were prepared by mixing the wheat rust pathogenic microbe and 5 mL 0.1 % dextrose solution evenly. Solutions of complex of different concentrations were prepared from the stock solutions by dilution complex in distilled water. A drop of mixed liquor of 2 mL suspensions and 2 mL stock solution was dripped on a concavity slide. The concavity slide were inverted on the keep-wet shelf and incubated for 24 h at 12 °C. The sprout number of the spore was counted if the germinal tube exceeds the half of the spore diameter.

DNA-binding study: The interaction of the yttrium(III) complex with DNA was investigated by absorption spectrum and fluorescence Absorption titration experiment was performed with fixed concentrations of the drugs (1.0×10^{-5} mol L^{-1}) while gradually increasing concentration of DNA. An excitation wavelength of 310 nm was used and total fluorescence emission intensity was monitored at 417 nm, which fixed amounts of compound were titrated with increasing amounts of DNA.

RESULTS AND DISCUSSION

Crystal structure: Single crystals of the compound were obtained from a mixed solution of ethanol and water after slow evaporation at room temperature [14]. It crystallizes in the triclinic system and space group P-1. A diagram of the crystal structure of complex is presented in Fig. 1. Important bond lengths and bond angles data are presented in Tables 1 and 2, respectively.

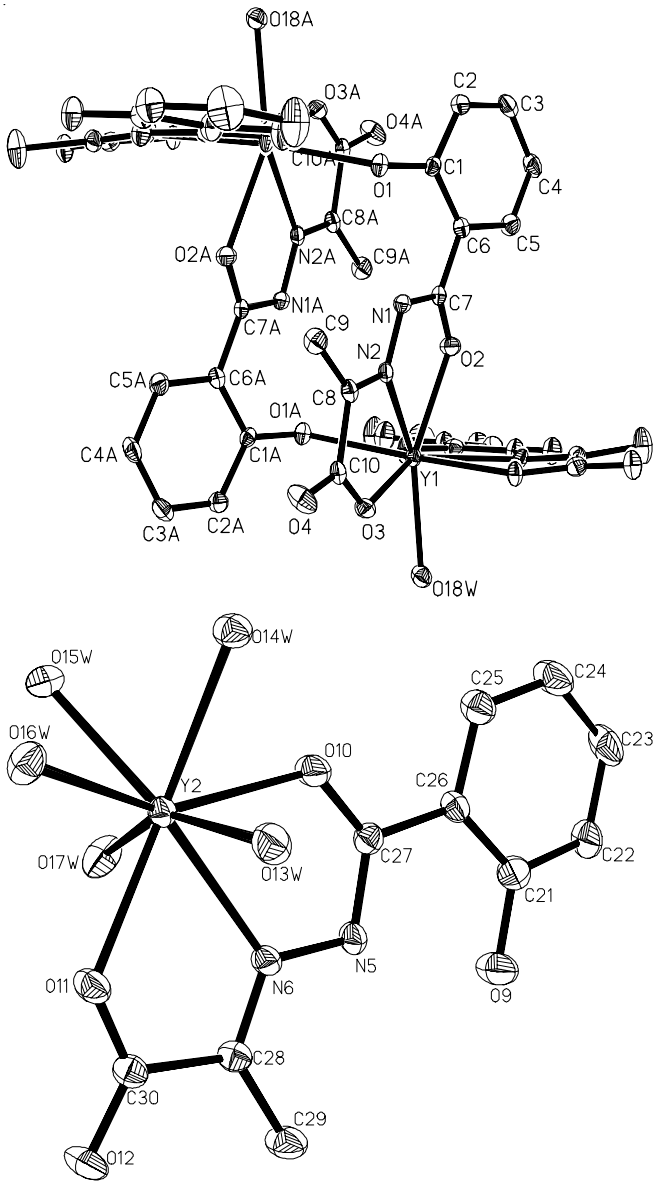

Fig. 1. Molecular structure of the complex (centrosymmetric unit). Ellipsoids are drawn at the 30 % probability level

X-ray structure analysis reveals that the complex exists two crystallographically independent molecules in the crystalline lattice (Fig. 1) and we found that this is the first yttrium(III) complex of N-(2-propionic acid)-salicyloyl hydrazone in two different coordination styles in the crystalline state. It contains a centrosymmetric unit (1) and an unattached unit. The centro-symmetric unit consists of two eight coordinated Y(III) center, four N-(2-propionic acid)-salicyloyl hydrazones and two water molecule. It is noticeably that there are two oxygen atoms of phenolic hydroxy were coordinated in the centro-symmetric unit and formed a big ring. In the unattached unit, Y(III) metal ion is surrounded by five oxygen atoms originating from five coordinated water molecules, two oxygen atoms and a nitrogen atom from the coordinated hydrazone ligand. There are three lattice water in the crystal lattice. The complex adopts a dodecahedron coordination geometry with the Y(III) metal ion. Due to the oxophilic character of lanthanide, the mean bond length of Y-O (2.327 Å) is shorter than that of Y-N (2.480 Å). Comparing with the distances of C-O (1.42

TABLE-1
IMPORTANT DATA OF BOND LENGTHS (Å)

Bond names	Bond lengths	Bond names	Bond lengths	Bond names	Bond lengths
Y(1)-O(1)#1	2.278(3)	Y(1)-O(6)	2.302(3)	Y(1)-O(2)	2.332(3)
Y(1)-O(3)	2.351(3)	Y(1)-O(7)	2.364(3)	Y(1)-O(18w)	2.403(4)
Y(1)-N(4)	2.486(3)	Y(1)-N(2)	2.505(4)	Y(2)-O(10)	2.276(3)
Y(2)-O(11)	2.324(3)	Y(2)-O(13w)	2.325(4)	Y(2)-O(16w)	2.346(4)
Y(2)-O(17w)	2.355(4)	Y(2)-O(15w)	2.358(4)	Y(2)-O(14w)	2.434(4)
Y(2)-N(6)	2.449(4)	O(1)-Y(1)#1	2.278(3)	O(2)-C(7)	1.250(5)
O(6)-C(17)	1.276(5)	O(10)-C(27)	1.276(6)	C(1)-O(1)	1.317(5)
C(11)-O(5)	1.341(6)	C(21)-O(9)	1.355(6)	N(1)-C(7)	1.363(5)
N(3)-C(17)	1.333(6)	C(27)-N(5)	1.329(6)	–	–

Symmetry transformations used to generate equivalent atoms: #1 -x,-y+2,-z+1

TABLE-2
IMPORTANT DATA OF BOND ANGLES (°)

Bond angles	Angle	Bond angles	Angle	Bond angles	Angle
O(1)#1-Y(1)-O(6)	75.97(11)	O(1)#1-Y(1)-O(2)	95.52(11)	O(6)-Y(1)-O(2)	80.60(12)
O(1)#1-Y(1)-O(3)	80.98(11)	O(6)-Y(1)-O(3)	145.73(11)	O(2)-Y(1)-O(3)	127.04(11)
O(1)#1-Y(1)-O(7)	155.13(11)	O(6)-Y(1)-O(7)	128.55(10)	O(2)-Y(1)-O(7)	85.96(11)
O(3)-Y(1)-O(7)	78.43(11)	O(1)#1-Y(1)-O(18w)	103.37(12)	O(6)-Y(1)-O(18w)	82.61(12)
O(2)-Y(1)-O(18w)	150.80(11)	O(3)-Y(1)-O(18w)	78.44(11)	O(7)-Y(1)-O(18w)	86.04(12)
O(1)#1-Y(1)-N(4)	139.32(12)	O(6)-Y(1)-N(4)	64.14(12)	O(2)-Y(1)-N(4)	71.30(11)
O(3)-Y(1)-N(4)	137.98(12)	O(7)-Y(1)-N(4)	64.49(11)	O(18w)-Y(1)-N(4)	79.91(12)
O(1)#1-Y(1)-N(2)	77.78(11)	O(6)-Y(1)-N(2)	132.56(12)	O(2)-Y(1)-N(2)	63.44(11)
O(3)-Y(1)-N(2)	64.23(11)	O(7)-Y(1)-N(2)	80.78(11)	O(18w)-Y(1)-N(2)	142.14(12)
N(4)-Y(1)-N(2)	124.06(12)	O(10)-Y(2)-O(11)	129.26(12)	O(10)-Y(2)-O(13w)	88.33(14)
O(11)-Y(2)-O(13w)	81.62(13)	O(10)-Y(2)-O(16w)	146.93(13)	O(11)-Y(2)-O(16w)	78.50(13)
O(13w)-Y(2)-O(16w)	77.51(15)	O(10)-Y(2)-O(17w)	85.87(15)	O(11)-Y(2)-O(17w)	82.18(14)
O(13w)-Y(2)-O(17w)	153.53(15)	O(16w)-Y(2)-O(17w)	119.29(15)	O(10)-Y(2)-O(15w)	101.68(13)
O(11)-Y(2)-O(15w)	119.04(13)	O(13w)-Y(2)-O(15w)	137.40(14)	O(16w)-Y(2)-O(15w)	71.75(14)
O(17w)-Y(2)-O(15w)	69.05(14)	O(10)-Y(2)-O(14w)	69.26(12)	O(11)-Y(2)-O(14w)	147.74(13)
O(13w)-Y(2)-O(14w)	72.01(14)	O(16w)-Y(2)-O(14w)	77.93(13)	O(17w)-Y(2)-O(14w)	128.90(15)
O(15w)-Y(2)-O(14w)	73.25(13)	O(10)-Y(2)-N(6)	64.38(12)	O(11)-Y(2)-N(6)	65.00(12)
O(13w)-Y(2)-N(6)	82.13(14)	O(16w)-Y(2)-N(6)	140.33(14)	O(17w)-Y(2)-N(6)	72.08(14)
O(15w)-Y(2)-N(6)	139.55(13)	O(14w)-Y(2)-N(6)	126.95(13)		

Symmetry transformations used to generate equivalent atoms: #1 -x,-y+2,-z+1

Å) and C=O (1.23 Å), the bond lengths of O(2)-C(7), O(10)-C(27) and O(6)-C(17) are 1.250, 1.276 and 1.276 Å, indicating that these bonds are doublelinkage and the ligand functions as a keto form.

There are abundant hydrogen bonds in the molecule. The data of hydrogen bonding in these structures are presented in Table-3. The intramolecular hydrogen bonds contain three types: one is formed between nitrogen atom of amido and oxygen atom of the phenol hydroxyl (N(1)-H(1)···O(1), O(5)-H(5)···N(3)), another is formed between oxygen atoms of coordinated water and lattice water (O(17W)-H(17B)···O(21W), O(17W)-H(17A)···O(20W), the third is formed between oxygen atoms of coordinated water and carboxyl (O(15W)-H(15A)···O(8)). All water molecules are linked with the ligand by hydrogen bonds. And all the other hydrogen bonds are intermolecular hydrogen bonds. The abundant hydrogen bonds not only make the crystal formed three dimensional network but also provide an extra stability for the crystal.

IR spectra: The significant IR absorption bands of the ligand and its complexes are presented in Table-4. IR spectra of the complex and the ligand (H_3L) are identified according to references [15]. The bands appearing in the infrared spectra of the free ligand (H_3L) at 3277, 1642, 1755, 1639, 1532, 1290 cm^{-1} are assigned to ν(N-H), ν(C=N), ν(COOH), amine I ν(C=O), amine II δ(NH), amine III [ν(C-N) + δ(NH)], respectively. The complex shows a strong IR band at 1605 cm^{-1} assigned to ν(C=N) vibration, which indicates that the C=N was coordinated. The absence of amine I ν(C=O) (1639 cm^{-1}) in the complex points to the coordination of the C=O group. The characteristic absorptions of the complex at 1619 and 1361 cm^{-1} related to $\nu_{as}(COO^-)$ and $\nu_s(COO^-)$ stretching vibration, respectively. The $\Delta\nu(\nu_{as}-\nu_s)$ is 258 cm^{-1} and this indicate that the complex adopt unidentate carboxylate structure. The intensity of the ν(OH) (ArOH) (3600 cm^{-1}) and amine II δ(NH) decreased, which suggest that the hydrogen of ArOH and -NHN- is partly lost. The amine III [ν(C-N) + δ(NH)] is split up into two bands at 1251 and 1344 cm^{-1}. In the complex, there are also a new wide band of water vibration at 3406 cm^{-1} and the in-plane and out-of-plane vibration of water at 763 and 586 cm^{-1} which are associated with the coordinated water. These conclusions are supported by the results of X-ray diffraction studies.

Growth rate method experiment of the complex: Two pathogenic bacteria: *Botrytis cirerea Pers.ex Tris*. and *Alternaria alternata Fries keissler* were used to test the bioactivity of the ligand and its complex according to growth rate method. The results were summarized in Table-5. It can clearly seen from Table-5 that the inhibitory rate of the complex was 100 % against *Botrytis cirerea Pers. ex Tris*. and *Alternaria alternata*

TABLE-3
HYDROGEN BONDS FOR THE COMPLEX (Å AND °)

D-H···A	d(D-H)	d(H···A)	d(D···A)	∠(DHA)
O(19W)-H(19E)···O(4)#1	0.851(10)	2.10(8)	2.745(6)	132(9)
O(15W)-H(15A)···O(8)	0.850(10)	1.93(2)	2.745(5)	161(6)
O(17W)-H(17B)···O(21W)	0.851(10)	1.863(17)	2.703(6)	169(7)
O(17W)-H(17A)···O(20W)	0.847(10)	2.024(19)	2.849(6)	164(5)
O(14W)-H(14A)···O(18W)#2	0.850(10)	2.224(2)	3.066(6)	171(8)
O(13W)-H(13B)···O(19W)#3	0.846(10)	1.837(14)	2.679(6)	173(6)
O(19W)-H(19D)···O(12)#4	0.852(10)	1.998(17)	2.842(6)	171(8)
O(13W)-H(13A)···O(20W)#2	0.845(10)	1.910(14)	2.751(6)	173(6)
O(16W)-H(16B)···O(11)#5	0.849(11)	1.896(17)	2.737(5)	171(8)
O(16W)-H(16A)···O(19W)#6	0.851(10)	2.66(6)	3.064(7)	111(5)
O(16W)-H(16A)···O(4)#2	0.851(10)	2.18(2)	3.005(6)	164(6)
O(18W)-H(18A)···O(5)#7	0.847(10)	1.872(13)	2.713(5)	172(5)
O(18W)-H(18B)···O(8)#8	0.847(10)	1.988(15)	2.825(5)	169(5)
O(21W)-H(21B)···O(12)#9	0.847(10)	1.916(13)	2.760(5)	174(5)
O(21W)-H(21A)···O(7)	0.843(10)	1.99(2)	2.782(5)	155(4)
O(20W)-H(20B)···O(10)#8	0.848(10)	2.65(4)	3.352(6)	141(5)
O(20W)-H(20A)···O(9)#10	0.845(10)	1.99(3)	2.769(6)	153(5)
O(15W)-H(15B)···O(3)#2	0.850(10)	1.919(13)	2.766(5)	174(6)

Symmetry transformations used to generate equivalent atoms:
#1 -x,-y+2,-z+1 #2 x+1,y, z #3 x+1,y, z+1 #4 x, y, z-1 #5 -x+2,-y+2,-z+2
#6 -x+1,-y+2,-z+1 #7 -x,-y+1,-z+1 #8 x-1,y,z #9 -x+1,-y+2,-z+2 #10 -x+1,-y+1,-z+2

TABLE-4
SOME MAIN IR DATA OF THE LIGAND AND THE COMPLEX

	ν(N-H)	ν(C=N)	ν(COOH)	Amine I	Amine II	Amine III	$\nu_{as}(COO^-)$	$\nu_{s}(COO^-)$	ν(OH)
H_3L	3277	1642	1755	1639	1532	1290	–	–	3600
Complex	3275	1605	–	–	1539	1251, 1344	1619	1361	3600

TABLE-5
ANTIMICROBIAL ACTIVITY FOR COMPLEX BY GROWTH RATE METHOD

Concentration (μg/mL)	*Botrytis cirerea Pers.ex Tris.* Inhibitory rate (%)	*Alternaria alternata Fries keissler* Inhibitory rate (%)
160	100	100
80	100	100
40	78	100
20	72	44
10	70	28

TABLE-6
ANTIMICROBIAL ACTIVITY FOR *Puccinia striiformis Westendorp* BY SPORE SPROUT METHOD

Concentration (μg/mL)	Average sprout rate (%)	Inhibitory rate (%)
250	0	100.0
25	2.67	97.2
2.5	15.3	83.8
0.25	69.3	26.5
0.025	89.7	4.9
Blank	94.3	–

Fries keissler at 80 and 40 μg/mL, respectively, while the inhibitory rate of the ligand only had 43.2 % against *Alternaria alternata Fries keissler* and nearly no effect against the other bacteria at 2500 μg/mL. With the decrease of concentration grade for the complex, the inhibition effect lessened step by step. In addition, it was noticeable that when the concentration decreased to 10 μg/mL, the inhibitory rate against *Botrytis cirerea Pers. ex Tris* still had 70 %.

Spore sprout method experiment of the complex: The results of the complex against *Puccinia striiformis Westendorp* were listed in Table-6. In general, the compound had showed the most potent antibacterial activity against *Puccinia striiformis Westendorp.* The inhibitory rate had reached 100 % when the concentration was 250 μg/mL. With the concentration of the complex decreasing, the inhibitory rate fell gradually. In the concentration range of 250-2.5 μg/mL, the decreasing amplitude of the inhibitory rate was quite slowly. When the concentration less than 2.5 μg/mL, the antibacterial activity decreased sharply from 83.8 to 4.9 %. It is obvious that the effective concentration of the complex is no less than 2.5 μg/mL. That is to say, when the complex was used to cure the wheat disease caused by *Puccinia striiformis Westendorp* in the future, only a small quantity of it is enough. In addition, the price of yttrium is much cheaper than the other rare earth. Considering all of the above, the complex should have good application in agriculture.

UV-visible absorption spectroscopy: The binding of the complex to DNA has also been characterized classically through absorption titration. The absorption spectra of the complex in the absence and presence of calf thymus-DNA are shown in Fig. 2. It is interesting to find that the intensity of the absorption band at 282 and 327 nm increased dramatically upon addition of calf thymus-DNA and the hyperchromicity were 82.91 and 123.82 % and the one at 327 nm also presented red-shift. This spectra change process reflects the corresponding changes of DNA in its conformation and structures after the drug bound to DNA [16]. The reason that the absorption intensity were increased may have been be largely due to the

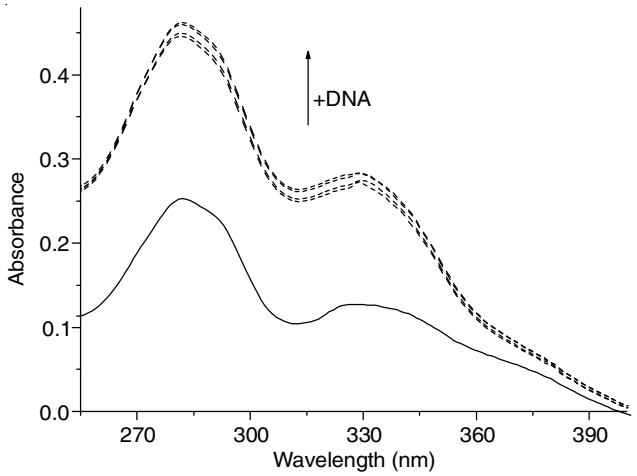

Fig. 2. Electronic absorption spectra of the complex (1.0×10^{-5} mol L^{-1}) in the absence and presence of calf thymus-DNA. Arrow shows the absorbance upon increasing DNA concentration

fact that the purine bases and pyrimidine bases of DNA were exposed because of the binding of the complex to DNA [17]. The similar hyperchromism has been observed for the sorest bands of certain porphyrins when interacted with DNA but has not yet been clearly explained [18]. However, the exact binding modes can be defined only if the crystal structures of the complex-oligonucleotide adducts are determined [19]. So the exact mode of interaction remains to be defined.

Luminescence studies: To get further insight into the nature of interactions between the title compound and DNA, we have additionally applied the fluorescence measurements. The complex has luminescence in Tris buffer at room temperature with maximum at 417 nm. Upon addition of DNA, the emission intensities of the compound grow to around 1.49 times as shown in Fig. 3. With adding calf thymus DNA solution to the title compound solution, enhanced fluorescence was observed and with a quite slightly wavelength shift at the same time. It suggested that the strong enhancement may be largely due to

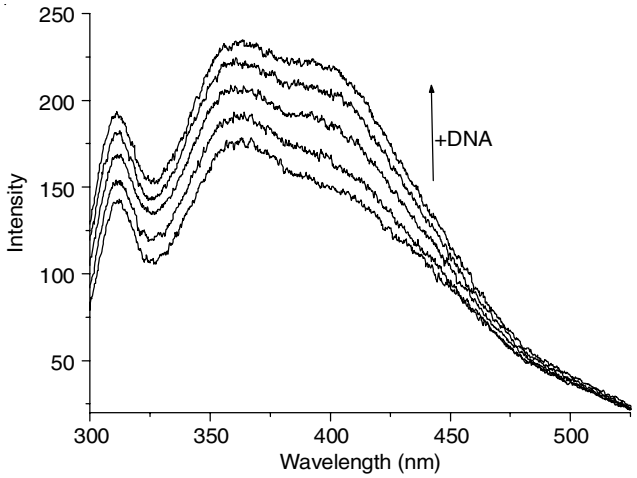

Fig. 3. Emission enhancement spectra of the complex (1.0×10^{-5}mol L^{-1}) in the presence of calf thymus-DNA. Arrow shows the emission intensities changes upon increasing DNA concentration

the interaction between adjacent base pairs of calf thymus-DNA and the small molecules bound into them [17]. The increase of the molecule's planarity and the decrease of the collisional frequency solvent molecules with the complexes usually leads to emission enhancement. So the complex may be intercalate into adjacent base pairs of DNA.

Conclusion

The novel yttrium(III) complex of N-(2-propionic acid)-salicyloyl hydrazone were prepared in good yields and characterized by a range of spectroscopic techniques. The X-ray crystal structure reveals that the title compound is the first yttrium(III) complex of N-(2-propionic acid)-salicyloyl hydrazone in which the ligand has two different coordinate patterns in the crystalline state. This novel yttrium N-(2-propionic acid)-salicyloyl hydrazone compound has showed strong antimicrobial activity against *Botrytis cirerea Pers.ex Tris.*, *Alternaria alternata Fries keissler* and *Puccinia striiformis Westendorp*. Moreover, the compound can also interact with calf thymus-DNA obviously.

ACKNOWLEDGEMENTS

This work is financially supported by the National Natural Science Foundations of China (No. 21273171) and Technology Plan Projects of Shangluo (No. SK2014-01-09).

REFERENCES

1. B.Y. Wu, L.H. Gao, Z.M. Duan and K.Z. Wang, *J. Inorg. Biochem.*, **99**, 1685 (2005).
2. K.E. Erkkila, D.T. Odom and J.K. Barton, *Chem. Rev.*, **99**, 2777 (1999).
3. C. Metcalfe and J.A. Thomas, *Chem. Soc. Rev.*, **32**, 215 (2003).
4. A. Silvestri, G. Barone, G. Ruisi, M.T. Lo Giudice and S. Tumminello, *J. Inorg. Biochem.*, **98**, 589 (2004).
5. L.M. Wilhelmsson, F. Westerlund, P. Lincoln and B. Norden, *J. Am. Chem. Soc.*, **124**, 12092 (2002).
6. C. Denison and T. Kodadek, *Chem. Biol.*, **5**, R129 (1998).
7. Z.Y. Yang, B.D. Wang and Y.H. Li, *J. Organomet. Chem.*, **691**, 4159 (2006).
8. B.D. Wang, Z.Y. Yang and T.R. Li, *Bioorg. Med. Chem.*, **14**, 6012 (2006).
9. M.A. Mesubi and B.A. Omotowa, *Synth. React. Inorg. Met.-Org. Chem.*, **23**, 435 (1993).
10. N.P. Buu-Hri, M.D. Xuong, N.H. Nam, F. Binon and F. Royer, *J. Chem. Soc.*, 1358 (1953).
11. J.K. Sears and J.R. Darby, The Technology of Plasticizers, Wiley, New York (1982).
12. E. Massarani, D. Nardi, A. Tajana and L. Degen, *J. Med. Chem.*, **14**, 633 (1971).
13. F.-Y. Chen, W.-K. Cao, X.-R. Liu, K. Peng, S.Y. He, R.X. Wang and Q.Z. Shi, *Synth. React. Inorg. Met.-Org. Chem.*, **36**, 569 (2006).
14. F.Y. Chen, S.Y. He, X.R. Liu, W.T. Wu and F. Liu, *Acta Crystallogr.*, **E63**, m468 (2007).
15. G.B. Deacon, *J. Coord. Chem. Rev.*, **33**, 227 (1980).
16. Q.S. Li, P. Yang, H.F. Wang and M.L. Guo, *J. Inorg. Biochem.*, **64**, 181 (1996).
17. Y.M. Song, Q. Wu, P.J. Yang, N.N. Luan, L.F. Wang and Y.M. Liu, *J. Inorg. Biochem.*, **100**, 1685 (2006).
18. R.F. Pasternack, E.J. Gibbs and J.J. Villafranca, *Biochemistry*, **22**, 2406 (1983).
19. J. Liu, T.X. Zhang, T.B. Lu, L.H. Qu, H. Zhou, Q.L. Zhang and L.N. Ji, *J. Inorg. Biochem.*, **91**, 269 (2002).